Ghosting reduction in scene-based nonuniformity correction of infrared image sequences

Junqi Bai (白俊奇), Qian Chen (陈 钱), Weixian Qian (钱惟贤), and Xianya Wang (王娴雅)*

441 Lab, School of Electronic Engineering and Optoelectronic Techniques, Nanjing University of Science and Technology, Nanjing 210094, China

**E-mail: xiaotuo1212@yahoo.com.cn*

Received May 24, 2010

Scene-based adaptive nonuniformity correction (NUC) is currently being applied to achieve higher performance in infrared imaging systems. However, almost all scene-based NUC algorithms cause the production of ghosting artifacts over output images. Based on constant-statistics theory, we propose a novel threshold self-adaptive ghosting reduction algorithm to improve the space low-pass and temporal high-pass (SLP-THP) NUC technique. The correction parameters of the previous frame are regarded as thresholds to compute new correction parameters. Experimental results show that the proposed algorithm can obtain a satisfactory performance in reducing unwanted ghosting artifacts.

OCIS codes: 040.3060, 100.2550, 100.2960, 100.2980.
doi: 10.3788/COL20100812.1113.

Infrared (IR) imaging systems have been widely used in both military and civilian fields. However, fixed pattern noise caused by nonuniform response of detectors is an intrinsic shortcoming of IR imaging. Nonuniformity correction (NUC) techniques were developed to perform the necessary calibration. Reference-based corrections using calibrated images on startup cannot solve the drift in the parameters of the detectors over time. As a result, scene-based corrections[1−3] have been studied to continuously correct IR nonuniformity without using references and interrupting detections. However, ghosting artifacts are major problems of scene-based NUC. The best known NUC technique based on temporal high-pass (THP) filters is highly dependent on object motion. If an object in the image moves slowly or remains stationary for a large number of iterations, it will cause the production of ghosting artifacts over the output images.

To reduce the ghost effect, Harris *et al.* proposed a simple de-ghosting module in constant-statistics NUC[3], wherein the correction parameters will not be updated until the changes of each pixel are greater than the threshold. Aiming at the NUC based on neural network[4], Esteban *et al.* presented two different adaptive learning rate strategies to reduce ghosting artifacts[5]. Recently, Qian *et al.* proposed an interesting space low-pass and THP (SLP-THP) NUC to eliminate ghosting artifacts[6]. In the abovementioned NUC techniques, a proper threshold is important to reduce ghosting artifacts effectively, but choosing the proper threshold is a very difficult task. The SLP-THP NUC was taken into consideration because using high threshold will not remove enough of the ghost artifacts, while using low threshold will cause few images for the estimation of correction parameters.

Aiming at the threshold problem of SLP-THP NUC, this letter proposes a novel threshold self-adaptive ghosting reduction NUC based on constant-statistics theory[7]. We adjust the threshold in our algorithm by using the correction parameters of the previous frame.

THP NUC is carried out by computing the difference between the input image and the temporal low-pass filter image, which can be expressed as

$$y(k) = x(k) - f(k), \tag{1}$$

$$f(k) = x(k)/N + (1 - 1/N) \times f(k-1), \tag{2}$$

where $x(k)$ is the input image, $y(k)$ is the output image, $f(k)$ is the average of $x(k)$ in the time domain, and N is the number of accumulable frames.

In THP NUC, correction parameters are estimated using the whole space frequency of the input image. In view of the space characteristic of nonuniformity (which mainly exists in high-space frequency of image, as shown in Fig. 1), SLP-THP NUC divides the space frequency of image into two parts: low-space frequency and high-space frequency.

Assuming $x = z + nu$, x is the input image, z is the original image, and nu is the nonuniformity. Hence, x, z, and nu can be expressed as

$$x(k) = x^{\mathrm{low}}(k) + x^{\mathrm{high}}(k), \tag{3}$$

$$z(k) = z^{\mathrm{low}}(k) + z^{\mathrm{high}}(k), \tag{4}$$

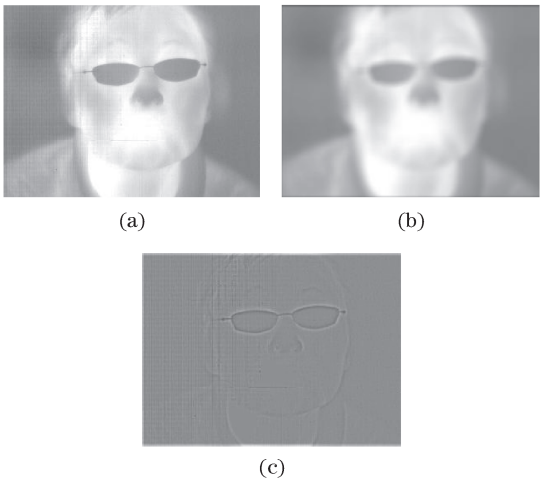

(a) (b) (c)

Fig. 1. Different space frequency images. (a) Input image; (b) low-space frequency; (c) high-space frequency.

$$nu(k) = nu^{\text{low}}(k) + nu^{\text{high}}(k), \tag{5}$$

where x^{low} and x^{high} are the low-space frequency and high-space frequency of x, respectively; z^{low} and z^{high} are the low-space frequency and high-space frequency of z, respectively; nu^{low} and nu^{high} are the low-space frequency and high-space frequency of nu; k is the frame number. x^{high} can be written as

$$x^{\text{high}}(k) = z^{\text{high}}(k) + nu^{\text{high}}(k). \tag{6}$$

Therefore, SLP-THP NUC can be written as

$$y(k) = x(k) - f^{\text{high}}(k), \tag{7}$$

$$f^{\text{high}}(k) = \frac{\sum_{l=k-N+1}^{k} x^{\text{high}}(l)}{N}, \tag{8}$$

$$x^{\text{high}}(k) = x(k) - x(k) * A, \tag{9}$$

where A is the 15×15 average filter, and $*$ is the convolution operator. In Eq. (8), the computation needs N frames memory space and cannot be applied in the real-time system. Hence, $f^{\text{high}}(k)$ can be improved as

$$f^{\text{high}}(k) = x^{\text{high}}(k)/N + (1 - 1/N) \times f^{\text{high}}(k-1). \tag{10}$$

To further reduce ghosting artifacts, SLP-THP NUC introduces a threshold to distinguish nonuniformity from object edges. It can be expressed as

$$X^{\text{high}}(k) = \begin{cases} x^{\text{high}}(k) & |x^{\text{high}}(k)| < \text{Th} \\ 0 & |x^{\text{high}}(k)| \geq \text{Th} \end{cases}, \tag{11}$$

where $X^{\text{high}}(k)$ only contains nonuniformity, $x^{\text{high}}(k)$ contains nonuniformity and object edges, and Th is the threshold.

In Eq. (11), a proper threshold Th can effectively reduce ghosting artifacts. Currently, it maintains fast convergence. However, selecting the proper threshold is difficult because of scene changes[8]. The constant-statistics theory gives a good hypothesis to solve the problem arising from fixed threshold by assuming that the temporal mean and standard deviation of each pixel are constant over time and space. Based on this theory, correction parameters f^{high} will become more accurate over time, so we can use $f^{\text{high}}(k-1)$ of previous frames to decide whether the current pixel will be used to compute $f^{\text{high}}(k)$. Hence, $X^{\text{high}}(k)$ can be written as

$$X^{\text{high}}(k) = \begin{cases} x^{\text{high}}(k) & |x^{\text{high}}(k)| < f^{\text{high}}(k-1) + a \\ 0 & |x^{\text{high}}(k)| \geq f^{\text{high}}(k-1) + a \end{cases}. \tag{12}$$

For the kth image, the process of our algorithm can be described as follows:

1) $x_{i,j}^{\text{high}}(k) = x_{i,j}(k) - x_{i,j}(k) * A$,

2) $X_{i,j}^{\text{high}}(k) = \begin{cases} x_{i,j}^{\text{high}}(k) & |x_{i,j}^{\text{high}}(k)| < f_{i,j}^{\text{high}}(k-1) + a \\ 0 & |x_{i,j}^{\text{high}}(k)| \geq f_{i,j}^{\text{high}}(k-1) + a \end{cases}$,

3) $f_{i,j}^{\text{high}}(k) = X_{i,j}^{\text{high}}(k)/N + (1 - 1/N) \times f_{i,j}^{\text{high}}(k-1)$,

4) $y_{i,j}(k) = x_{i,j}(k) - f_{i,j}^{\text{high}}(k)$,

where (i, j) is the space coordinate, and parameter a used for increasing convergence speed is a constant.

To test the performance of algorithms, $C(k)$ is defined as

$$C(k) = \frac{\sum_{i=1}^{M}\sum_{j=1}^{N}\{f_{i,j}(k) - f_{i,j}(R)\}}{M \times N}, \tag{13}$$

where $f(k)$ is the correction parameter of the kth image, $f(R)$ is the true correction parameters after R frames, M is the number of rows, and N is the number of columns. In this letter, we assume that R denotes the 500th frame image. Figures 2(a) and (b) show the convergence speed of different algorithms. The convergence speed of THP NUC is shown in Fig. 2(a). In Fig. 2(b), the pane curve denotes SLP-THP NUC without threshold, the plus curve denotes our threshold self-adaptive NUC, the circle curve denotes SLP-THP NUC with threshold 20, and the asterisk curve denotes SLP-THP NUC with threshold 10. As shown in Fig. 2, the precision of our proposed algorithm is better than SLP-THP NUC over time and space (after 400 frames). On the other hand, the smaller the threshold, the slower the convergence speed.

The kth correction parameters, $f^{\text{high}}(k)$, of different algorithms are shown in Fig. 3, where k=60, 120, and 180. The accumulable frame N=40. This figure shows that $f^{\text{high}}(k)$ of THP NUC contains more

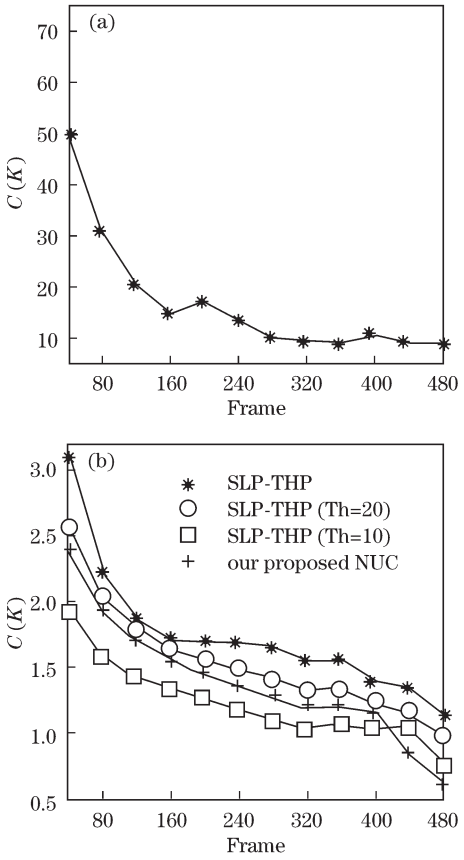

Fig. 2. Convergence speed of different algorithms. (a) THP NUC; (b) other NUC algorithms.

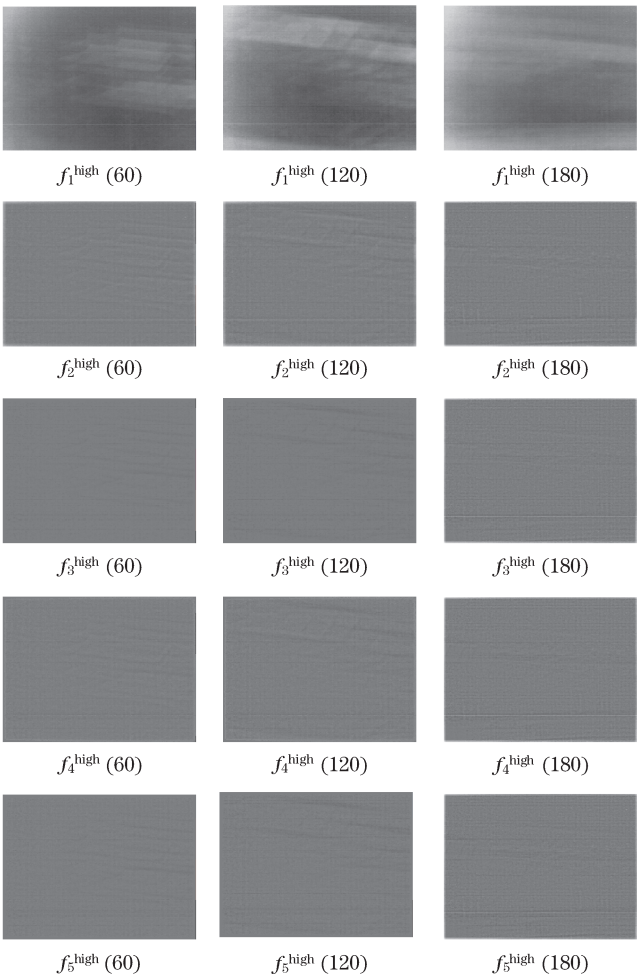

Fig. 3. Comparison of $f^{\text{high}}(k)$ of different algorithms. $f_1^{\text{high}}(k)$, $f_2^{\text{high}}(k)$, $f_3^{\text{high}}(k)$, $f_4^{\text{high}}(k)$, and $f_5^{\text{high}}(k)$ are the correction parameters of THP NUC, SLP-THP NUC without threshold, SLP-THP NUC with threshold 10, SLP-THP NUC with threshold 20, and our proposed NUC, respectively.

scene elements than the others. When k=60 or 120, the sequence of scene elements from more to less is $f_2^{\text{high}}(k)$, $f_4^{\text{high}}(k)$, $f_5^{\text{high}}(k)$, $f_3^{\text{high}}(k)$. When k=180, $f_2^{\text{high}}(180)$, $f_3^{\text{high}}(180)$, $f_4^{\text{high}}(180)$, and $f_5^{\text{high}}(180)$ have very few scene elements.

Figure 4 shows the correction performance of different algorithms, where k=80, except for Fig. 4(b). From this figure, obvious ghosting artifacts after THP NUC, such as the edge of house, are clearly seen. Compared with THP NUC, SLP-THP NUC without threshold can eliminate most of the ghosting artifacts. SLP-THP NUC with threshold further reduce the rest of ghosting artifacts, however, selecting the proper threshold is difficult. As shown in Fig. 4(e), a higher threshold is invalid to distinguish nonuniformity from object edges, the effect of which is similar to SLP-THP NUC without threshold. Figures 4(b) and (g) show the correction performance of Harris's constant-statistics algorithm using 500 frames of images and 80 frames of images, respectively. Performance results indicate that correction parameters of this algorithm cannot be precisely estimated using too few frames. Figure 4(h)

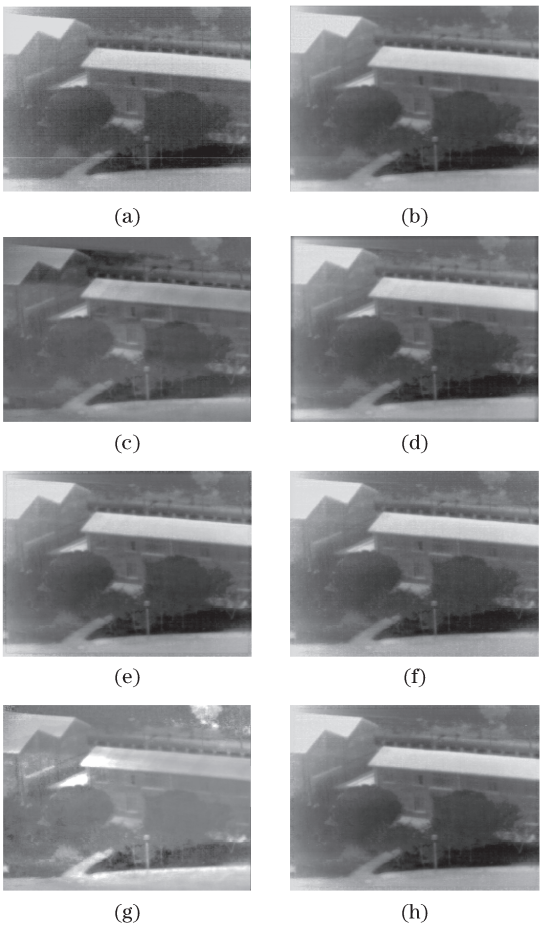

Fig. 4. Correction performance of different algorithms. (a) Original noise image; (b) constant-statistics NUC using 500 frames of images; (c) THP NUC; (d) SLP-THP NUC without threshold; (e) SLP-THP NUC with threshold 20; (f) SLP-THP NUC with threshold 10; (g) constant-statistics NUC using 80 frames of images; (h) our proposed NUC.

Table 1. MSE Comparison of Different NUC Algorithms (Fig. 4)

Image	(a)	(c)	(d)	(e)	(f)	(g)	(h)
MSE	5.34	40.92	10.43	4.04	3.37	48.81	2.52

shows our proposed de-ghosting NUC. The ghosting artifacts of the images are eliminated effectively because the threshold is computed self-adaptively using the correction parameters f^{high} of the previous frame.

To test the performance of different algorithms, mean square error (MSE) is used as the metric, which is defined as

$$\text{MSE}_k = E[(y_k - y_{\text{true}})^2]$$

where $E[\cdot]$ is the expected value operator, y_k is the kth corrected image, and y_{true} is the image without nonuniformity noise.

The original image sequences of real IR imaging system cannot be obtained without nonuniformity noise. Therefore, we regard the calibrated image Fig. 4(b) as the image y_{true}. The MSE comparison of different algorithms is shown in Table 1, which indicates that our proposed

NUC is better than the others.

In conclusion, a threshold self-adaptive de-ghosting NUC is proposed based on constant-statistics theory. The correction parameters of the previous frame are regarded as thresholds to compute current correction parameters. The proposed algorithm has been applied to real IR image sequences. Experimental results show that the process can reduce unwanted ghosting artifacts effectively.

The authors would like to acknowledge several discussions with Hassan Foroosh and Nazim Ashraf at the University of Central Florida. This work was supported by the Jiangsu Province Natural Science Foundation of China (No. BK2008049), the Colleges and Universities Innovation Projects (No. CX08B_045Z), and the Nanjing University of Science and Technology (NUST) Research Funding (No. 2010ZDJH12).

References

1. R. Lai, Y. Yang, B. Wang, H. Zhou, and S. Liu, Acta Opt. Sin. (in Chinese) **29,** 927 (2009).
2. H. Zhou, Y. Wei, H. Qian, and B. Wang, Acta Opt. Sin. (in Chinese) **29,** 378 (2009).
3. J. G. Harris and Y.-M. Chiang, Proc. SPIE **3377,** 106 (1998).
4. D. A. Scribner, K. A. Sarkady, M. R. Kruer, J. T. Caulfield, J. D. Hunt, and C. Herman, Proc. SPIE **1541,** 100 (1991).
5. V. R. Esteban and T. I. Sergio, in *Proceedings of IEEE International Conference on Image Processing* **2,** 1001 (2003).
6. W. Qian, Q. Chen, and G. Gu, Opt. Rev. **17,** 24 (2010).
7. J. G. Harris and Y.-M. Chiang, IEEE Trans. Image Process. **8,** 1148 (1999).
8. R. Charnigo, J. Sun, and R. Muzic, Jr., IEEE Trans. Image Process. **15,** 666 (2006).